(1)

Report Number: Motorola No 3404

High Frequency Wideband I.O. Bragg Cell

Dr. Fred Hickernell & Associates
Motorola Government Electronics Group
Aerospace Operations
8201 E. McDowell P.O. Box 1417
Scottsdale, Az 85252

December 20,1985

Final Report

Distribution NRL:6550;5720;DDC;6500;6502.2.

Prepared for:
Naval Research Laboratories [NRL]
4555 Overlook Avenue,SW
Washington,D.C. 20375

Monitored by:
Naval Research Laboratories

REPORT DOCUMENTATION PAGE

1a. REPORT SECURITY CLASSIFICATION Unclassified	1b. RESTRICTIVE MARKINGS No Proprietary Claims
2a. SECURITY CLASSIFICATION AUTHORITY NA	3. DISTRIBUTION/AVAILABILITY OF REPORT NA
2b. DECLASSIFICATION/DOWNGRADING SCHEDULE NA	
4. PERFORMING ORGANIZATION REPORT NUMBER(S) Motorola GEG No. 3404	5. MONITORING ORGANIZATION REPORT NUMBER(S) NRL 6570
6a. NAME OF PERFORMING ORGANIZATION Motorola, GEG, Inc. Aerospace Operations 6b. OFFICE SYMBOL (If applicable) NA	7a. NAME OF MONITORING ORGANIZATION Naval Research Laboratories
6c. ADDRESS (City, State and ZIP Code) 8201 E. McDowell P.O. Box 1417 Scottsdale, AZ 85252	7b. ADDRESS (City, State and ZIP Code) Naval Research Laboratory 4555 Overlook Ave., SW Washington, D.C. 20375
8a. NAME OF FUNDING/SPONSORING ORGANIZATION Naval Research Laboratory 8b. OFFICE SYMBOL (If applicable) 6570	9. PROCUREMENT INSTRUMENT IDENTIFICATION NUMBER Contract No. N00014-84-C-2447
8c. ADDRESS (City, State and ZIP Code) Naval Research Laboratory 4555 Overlook Ave., SW Washington, D.C. 20375	10. SOURCE OF FUNDING NOS PROGRAM ELEMENT NO.: 63206N, 64224N PROJECT NO.: W0639TW, W0617 TASK NO.: WORK UNIT NO.:
11. TITLE (Include Security Classification) Unclassified High Freq. Wideband IO Bragg Cell	
12. PERSONAL AUTHOR(S) Proj. Ldr. Dr. Fred Hickernell, Associates K.D. Ruehle, Dr. F. V. Richard	
13a. TYPE OF REPORT Final Report 13b. TIME COVERED FROM 9/84 TO 10/85	14. DATE OF REPORT (Yr., Mo., Day) 85 December 20 15. PAGE COUNT
16. SUPPLEMENTARY NOTATION NA	
17. COSATI CODES FIELD / GROUP / SUB. GR.	18. SUBJECT TERMS (Continue on reverse if necessary and identify by block number) IO Bragg Cell; GHz SAW Transducer; Proton Exchange; Titanium Indiffused Proton Exchange

19. ABSTRACT (Continue on reverse if necessary and identify by block number)

Reported are the results of a program to improve the high frequency acousto-optic diffraction efficiency of surface wave Bragg cells to extend the range of integrated optical spectrum analyzers. The acousto-optic performance of waveguides formed by the recently developed technique of proton exchanging lithium niobate (PE:$LiNbO_3$) was determined at frequencies in the 1 GHz region. Diffraction efficiencies of single transducer PE:$LiNbO_3$ Bragg cells were measured at 794, 893, 1021, and 1340 MHz and compared to titanium indiffused lithium niobate (Ti:$LiNbO_3$) results. Piezoelectric and elastic properties, along with optical loss and scatter characteristics, were determined for both annealed and unannealed PE:$LiNbO_3$ and titanium indiffused proton exchanged (TiPE:) $LiNbO_3$ waveguides.

20. DISTRIBUTION/AVAILABILITY OF ABSTRACT UNCLASSIFIED/UNLIMITED ☐ SAME AS RPT. ☒ DTIC USERS ☐	21. ABSTRACT SECURITY CLASSIFICATION Unclassified
22a. NAME OF RESPONSIBLE INDIVIDUAL Dr. Joseph Weller	22b. TELEPHONE NUMBER (Include Area Code) (202) 767-2768 22c. OFFICE SYMBOL NRL 6750

PREFACE

This report was prepared by Motorola Government Electronics Group, Scottsdale, Arizona, under Navy Contract Number N00014-84-C-2447, entitled "High Frequency Wideband IO Bragg Cell". Dr. Joe Weller, Naval Research Laboratory, is the Navy project engineer. This report presents the results of work performed between October 1984 to December 1985 in an effort to improve the performance of surface wave Bragg cells with respect to their high frequency diffraction efficiency. Dr. F.S. Hickernell, Principal Staff Engineer with the Integrated Circuit Facility, was the engineering project leader. The principal investigators were Mr. K.D. Ruehle and Dr. F.S. Hickernell.

Major support was provided by Ms. S.J. Joseph, Mr. C.T. Tegreene and Dr. C.M. Reese. Personnel who also contributed to the investigation included Dr. F.V. Richard, Dr. F.Y. Cho, Mr. J.R. Joseph and Mr. S. Bernsen.

Sincere appreciation is expressed to Ms. Debi Reynolds for her technical contributions pertaining to photolithographic transducer fabrication. The E-beam transducer fabrication performed by Mr. Phillip Seese and the transducer wirebonding done by Vi Huttie is gratefully acknowledged.

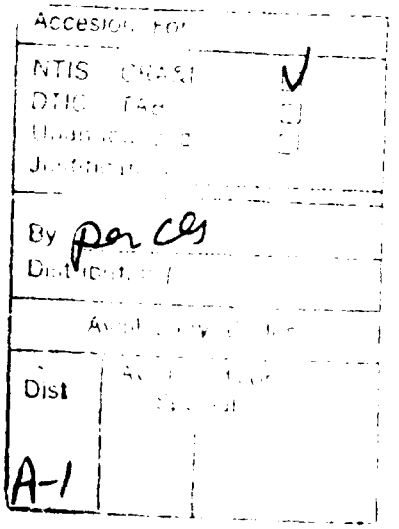

TABLE OF CONTENTS

LIST OF FIGURES

LIST OF TABLES

I. INTRODUCTION

1. STATEMENT OF PROBLEM

The acousto-optic spectrum analyzer will enable the realization of receivers with gigahertz bandwidth and megahertz resolution which would be applicable to CW or pulsed waveforms. The integrated optics approach combines surface acoustic wave (SAW) technology with guided wave optics to yield a compact, rugged, low cost device which would be virtually free of the precision alignment problems and components interface problems which compromise the performance of bulk acousto-optic devices. The heart of the integrated optical spectrum analyzer (IOSA) is the acousto-optic (AO) interaction between the SAW and the guided wave. If the AO interaction is optimum the IOSA can be driven at low powers thus reducing system constraints. Acousto-optic diffraction efficiency is a strong function of the physical overlap between the acoustic and optical fields. The penetration of the acoustic field into the crystal depends inversely on its frequency while the depth of the optical field is determined by the waveguide parameters.

The most common and well developed process of forming planar optical waveguides is the indiffusion of titanium into either lithium niobate ($LiNbO_3$) or lithium tantalate ($LiTaO_3$). In this type guide peak diffraction efficiency is obtained at acoustic frequencies in the 500 MHz region. Moreover, diffraction efficiency rolls off significantly above 1 GHz. The reason for this is the SAW now is very close to the crystal surface thus reducing the field overlap. Confinement of the optical field to a very narrow region along the surface would, in theory, produce better diffraction efficiency at high frequencies. This realization would allow applications of the IOSA to be extended into the gigahertz region. The primary objective here is to increase the high frequency acousto-optic diffraction efficiency of a surface wave Bragg cell by using waveguides that offer better optical confinement.

2. BACKGROUND

In order to confine the optical field close to the surface a large index difference, Δn is required between the waveguide and the

substrate. Figure 1 compares optical intensity for a single mode guide as a function of depth into the substrate for both titanium indiffused ($\Delta n=.01$) and proton exchanged ($\Delta n=.1$) lithium niobate. Waveguides formed by proton exchange guide light nearer the surface where the high frequency AO interaction occurs. The exchange of hydrogen ions (protons) for lithium ions in lithium niobate is refered to as proton exchange (PE). The reaction produces a decrease in the ordinary refractive index[1] and an increase in the extraordinary refractive index which is nonlinearly related to the proton concentration.[2] The proton exchange process produces a step refractive index profile which can be tailored by post annealing. The fact that n_e is increased allows the fabrication of waveguides whose modes are polarized to use the r_{33} electro-optic coefficient of lithium niobate. The use of r_{33} provides the highest figure of merit for electro-optic and acousto-optic interactions in lithium niobate. If the crystaline properties of the lithium niobate are not altered by the PE process, then it can be used to fabricate guided wave structures with optical field distributions tailored to optimize acousto-optic and electro-optic interactions.

Experimental evidence presented in the literature is somewhat inconclusive regarding proton exchange affecting lithium niobate crystal properties. A proton exchanged electro-optical frequency shifter demonstrated by Wong et al.[3] operated at voltages similar to a device made with a titanium indiffused waveguide. Geometrically identical Mach-Zehnder interferometers fabricated by proton exchange and titanium indiffusion were reported by Becker.[4] He concluded proton exchange definitely degraded the electro-optic activity and that the amount of degradation depended on the exchange time. Holman et al.[5] reported that, if anything, the electro-optic effect was enhanced by proton exchange. Korableu et al.[6] measured approximately the same acousto-optic diffraction efficiencies for proton exchange and titanium indiffused guides. Dawar et al.[7] used short exchanges and annealing to obtain acousto-optic diffraction efficiencies similar to Ti-indiffused results. More recently, Davis[8] observed significant reductions in the electro-mechanical coupling coefficient in proton exchange and accounted

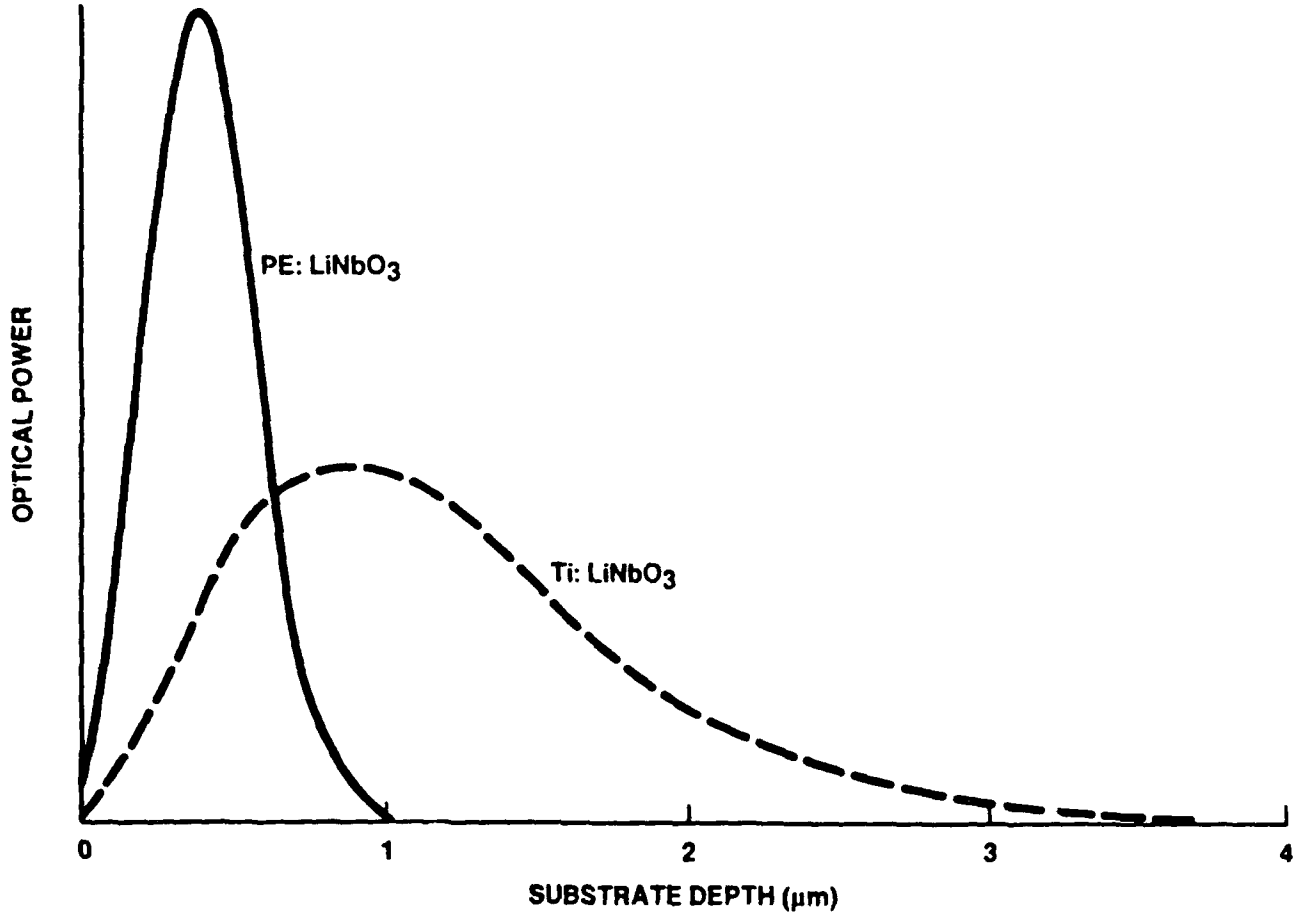

FIGURE 1. Optical confinement in single mode waveguides. Shown is a comparison of the optical intensity distribution in waveguides of titanium indiffused lithium niobate ($Ti:LiNbO_3$) and proton exchanged lithium niobate ($PE:LiNbO_3$).

for the drop in diffraction efficiency by concluding that the piezoelectrically induced fields and electro-optic coefficient, r_{33}, are reduced.

3. TECHNICAL APPROACH

The problem of obtaining good acousto-optic diffraction efficiency in a high frequency bragg cell were addressed, first, by emphasizing measurements of surface acoustic wave and guided optical wave properties of proton exchanged as compared to titanium indiffused lithium niobate. Then, the best transducer and waveguide processing techniques for proton exchanged substrates that optimize the acousto-optic interaction were identified.

a. Initial Waveguides

The initial waveguides were fabricated to provide both the highest TE_0 guided mode index and single mode operation. This combination gives the maximum guided optical wave confinement near the crystal surface for efficient interaction with the high frequency SAW. The acoustic, optical, and acousto-optic properties of these guides were measured. High acoustic losses, poor quality waveguides, and low AO diffraction efficiencies prompted an alternate approach for waveguide fabrication.

b. Alternate Approach

Efficient Bragg cell performance can be realized only if acoustic and optical losses are minimized. Most of the additional acoustic loss introduced by proton exchange was attributed to electro-mechanical coupling loss. This loss was eliminated by selectively exchanging only the AO interaction region and not the region under the SAW transducers. Large optical losses and heavy in-plane and out-of-plane scatter in the original guides were improved by three alternative fabrication procedures. The initial high (guided wave) index waveguides were annealed to low index; low index guides were fabricated and then annealed; and low index unannealed guides were investigated.

In addition, waveguides formed by proton exchanging titanium

indiffused (TiPE) substrates were examined to determine acoustic performance and optical quality. The original and the three alternative fabrication procedures outlined above were used to form TiPE guides. This allowed a complete matrix of PE and TiPE waveguide types to be evaluated and optimal fabrication parameters determined.

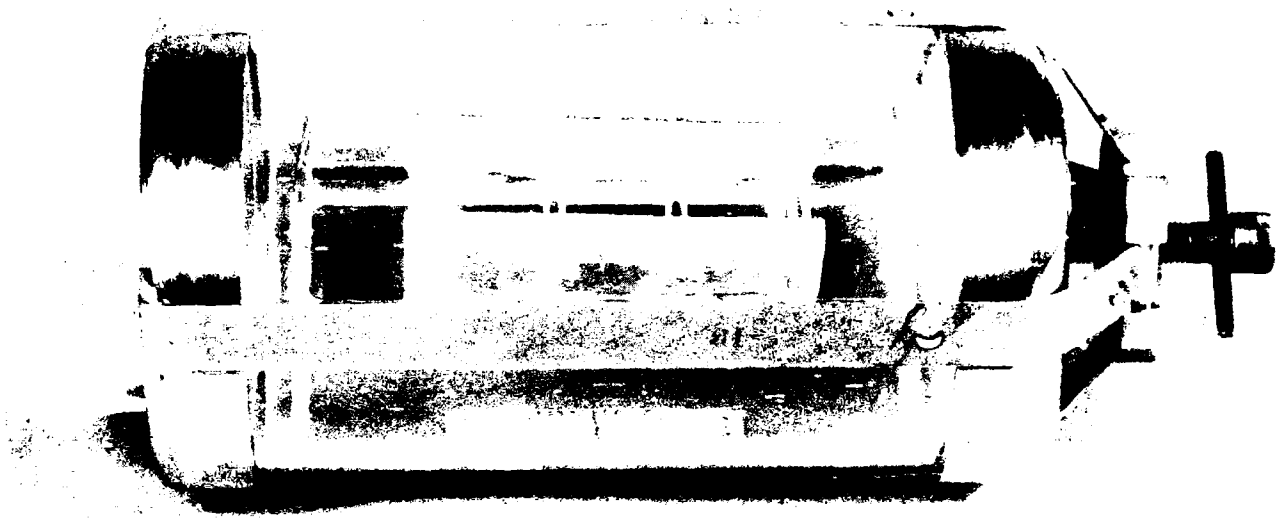

84-7485

53221-2

FIGURE 2. Cylindrical quartz ampoule used to proton exchange $LiNbO_3$. Substrates are emersed in a benzoic acid solution at 245°C contained in the ampoule.

II. WAVEGUIDE PROCESSING

1. PROTON EXCHANGE TECHNIQUE

a. Procedure

Waveguide fabrication was performed in a diffusion tube furnace using a cylindrical quartz ampoule (Figure 1) and the following procedure. A benzoic acid solution fills the bottom 1/3 of the cylinder lying on its side while Y-cut $LiNbO_3$ substrates sit in a quartz boat above the melt. The acid is brought up to 245°C and then rotated 180° degrees such that the substrates are immersed in the melt. A partial substitution of H^+ ions from the acid for Li^+ ions begins at the substrate surface and extends into the crystal at depths proportional to the square root of the diffusion time. When the run is complete, the ampoule is rotated another 180° and the substrates can cool out of the melt. Subsequently, the waveguides are ultrasonically cleaned in a propanol bath and blown dried with nitrogen.

b. Buffered Solutions

The advantages of mixed melts of lithium benzoate and benzoic acid have been reported in the literature.[1,2] Although exchange in benzoic acid alone is the simplest technique, it has disadvantages of etching y-cut plates, higher optical loss and scatter, and index instabilities. Adding small amounts of lithium benzoate to the melt produces guides with better optical properties and stability but also decreases the diffusion constant significantly. Unless otherwise specified, all guides were fabricated using a solution consisting of 97.5 M% benzoic acid and 2.5 M% lithium benzoate. Single and dual mode guides were fabricated in 4 to 7 hours. Multimode guides were exchanged for approximately 24 hours. Due to the long exchange times, a few guides were made with 1M% lithium benzoate. The short term optical and acoustic properties of these guides were indistinguishable from the 2.5 M% guides.

c. Diffusion Parameters

In order to establish diffusion parameters such as surface index and diffusion constant it was necessary to fabricate multimode waveguides. Guided mode indices are measured using standard prism coupling techniques and index profile were determined using an inverse-WKB method. From

these profiles the surface index and diffusion constant for a 2.5 M% solution were found to be 2.308 and 0.020 μm^2/hr respectively. These values compare favorably with the literature.[1]

2. INITIAL WAVEGUIDES

The initial approach focused on fabrication and evaluation of deep single mode and dual mode waveguides. With 2.5 M% guides this corresponds to waveguide depths of 0.55 to 0.85 microns. The best optical confinement for single mode operation is realized at the second order mode cutoff depth (.64 microns). Also, when the second order mode is present an improvement of the optical quality is observed. Therefore, both single and dual mode guides were fabricated and evaluated.

3. ALTERNATE APPROACH

After the evaluation of the above mentioned waveguides an extensive effort was made to improve their acoustic and optical properties. Acoustic insertion loss was improved by selectively exchanging only the region of optical propagation and the acousto-optic interaction and not the region under the SAW transducers (section IV.1.).

Also, a combination of titanium indiffusion and proton exchange (TiPE) guides were fabricated to improve waveguide quality. A 200Å layer of titanium was RF sputtered on and then indiffused into lithium niobate using the profile shown in Figure 2. The two-hour period at 500°C was designed to thoroughly oxidize the titanium prior to diffusion. The typical diffusion period was 2 hours and 10 minutes. The effective diffusion time is somewhat longer due to time spent on the up and down ramp portions of the cycle near the diffusion temperature. The proton exchange followed within a week of titanium indiffusion. The exact proton exchange diffusion parameters (diffusion constant and extraordinary surface index) in titanium indiffused lithium niobate were not established, although, they were observed to be similar to standard proton exchange. Many types of TiPE waveguides were fabricated, including high index, high index annealed to low index, low index annealed, and low index unannealed.

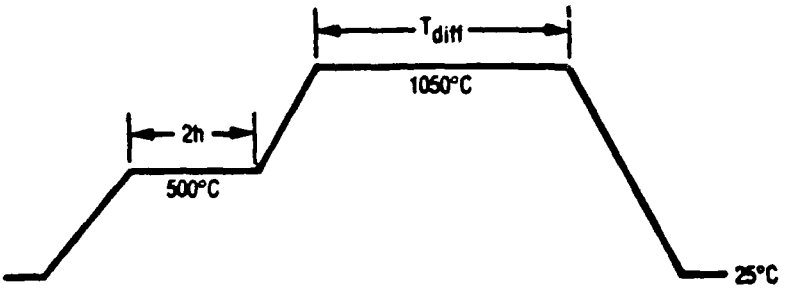

FIGURE 3. Diffusion profile for fabrication of Ti:$LiNbO_3$ waveguide.

III. WAVEGUIDE EVALUATION

1. OPTICAL MEASUREMENT TECHNIQUES

The optical guided wave index and propagation loss were determined on the proton exchanged and titanium-indiffused proton-exchanged, Y-cut lithium niobate planar waveguides. The measurements were made at 633 nm with a HeNe laser and at 832 nm with a GaAlAs diode laser using the following procedures. The extraordinary index change and the guided mode index are found by a standard mode line (m-line) measurement. This technique determines the propagation angle (zig-zag angle) of TE polarized wave traveling along the x-axis of PE:$LiNbO_3$. The optical loss and scattering properties of the waveguide are determined primarily by direct visual observation of the intensity and shape of the propagating beam (light streak) in the waveguide. A second prism is used to couple out the propagating beam when quantitative measurements of loss and scatter are required.

The m-line measurements are performed by focusing the beam on the contact point of the base of a rutile prism and the waveguide which couples a guided mode into the waveguide. The reflected beam is projected on a screen and allows for accurate mode line centering. The beam can be stopped down to a small diameter, the absorbed mode line centered, and the entrance angle measured to within one minute. Assuming that the indices of the rutile prism are accurate to four places the mode indices can be determined to $\pm$.0005.

For multimode guides the mode indices can be used to calculate the index profile of the waveguide region using an inverse-WKB approximation technique. Figure 4 shows a typical example of the step index profile characteristic of proton exchanged waveguides. From this plot, the surface index and exchange depth are found. Since a step index region is formed, it is also possible to calculate the approximate bulk refractive index and depth of the PE:$LiNbO_3$ region by using the slab waveguide model commonly used for film layers. When waveguides were deep enough to allow several modes to propagate this technique was checked against the WKB method and proven valid. Table 1 lists the index and thickness values of five representative samples to determine the consistency

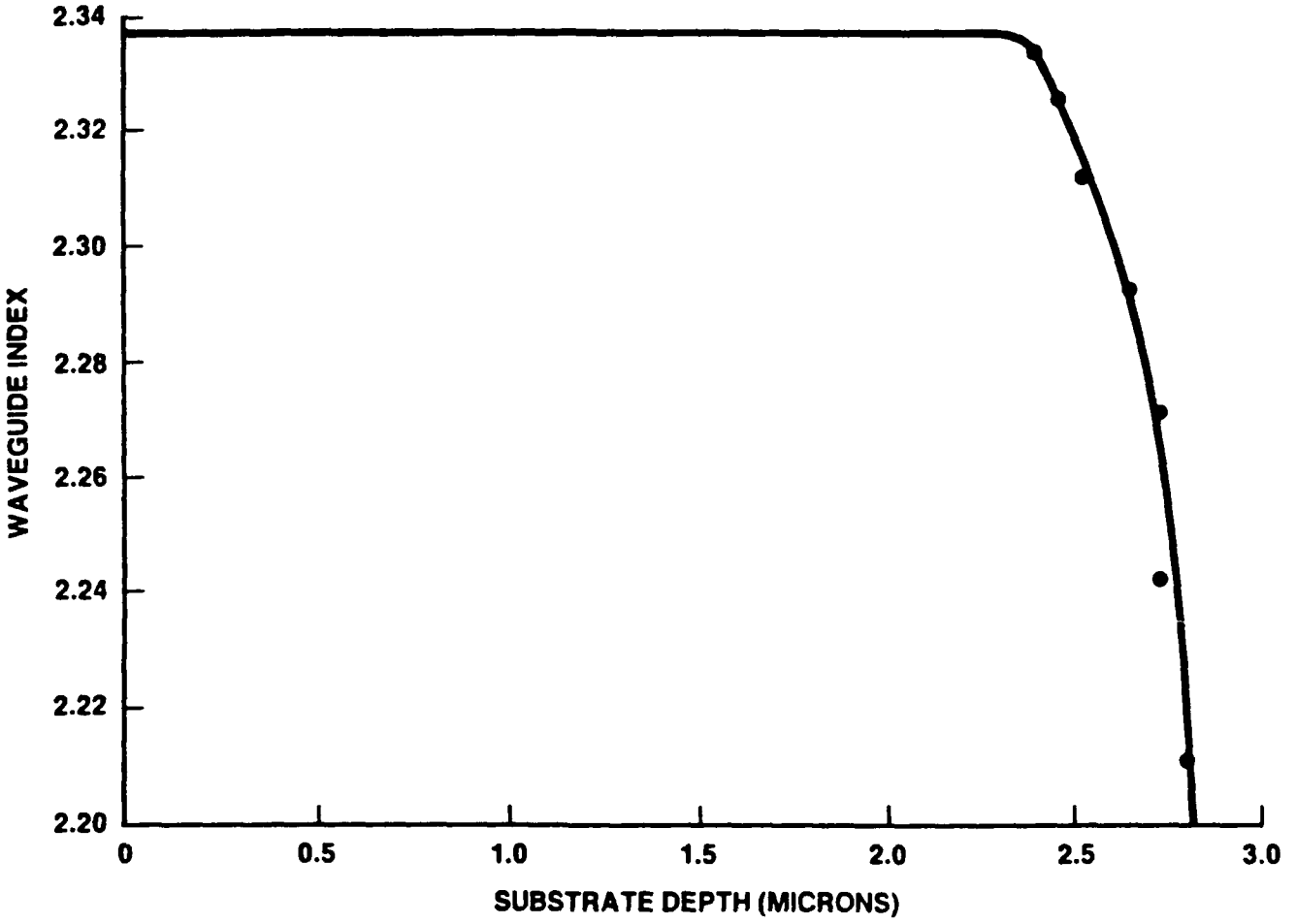

FIGURE 4. Typical index profile of waveguides formed by proton exchange. The waveguide index versus depth into the substrate is calculated from measurements of guided mode indices.

between the two techniques. The planar technique returns a slightly lower index value, although the difference is less than .5%. The difference in thickness varies from about 1% to 4% with the WKB method giving the lower value. The thickness of the guide using the WKB plot was taken to be at the point where the index dropped approximately 85%.

TABLE 1

PE:$LiNbO_3$ Index and Thickness Comparison
using the WKB and Film Methods

	WKB		FILM	
SAMPLE NUMBER	INDEX	THICKNESS (μm)	INDEX	THICKNESS (μm)
1	2.313	4.04	2.308	4.13
2	2.312	3.54	2.309	3.51
3	2.310	2.65	2.308	2.71
4	2.318	2.09	2.312	2.09
5	2.309	1.96	2.299	2.03

For shallow PE:$LiNbO_3$ waveguides supporting from 1 to 3 modes neither of the above methods are accurate. Instead, the guided mode index was measured and the proton exchanged thickness determined using mode dispersion diagrams like that shown in Figure 5. Dispersion curves were calculated by modeling the proton exchanged region as a perfect step index waveguide and using measured values of surface index and substrate index. Good accuracy was achieved by maintaining tight parameter controls on the proton exchange process. This produced waveguides with a known surface index allowing an accurate thickness determination. The dispersion diagram shown proved accurate at depths where multimode samples could be used for verification.

In most cases, loss and scatter levels were visually determined and compared to titanium indiffused waveguides. However, Figure 6 shows a quantitative measurement of loss using the moving two prism technique made on a dual guide. A linear least square fit determined the

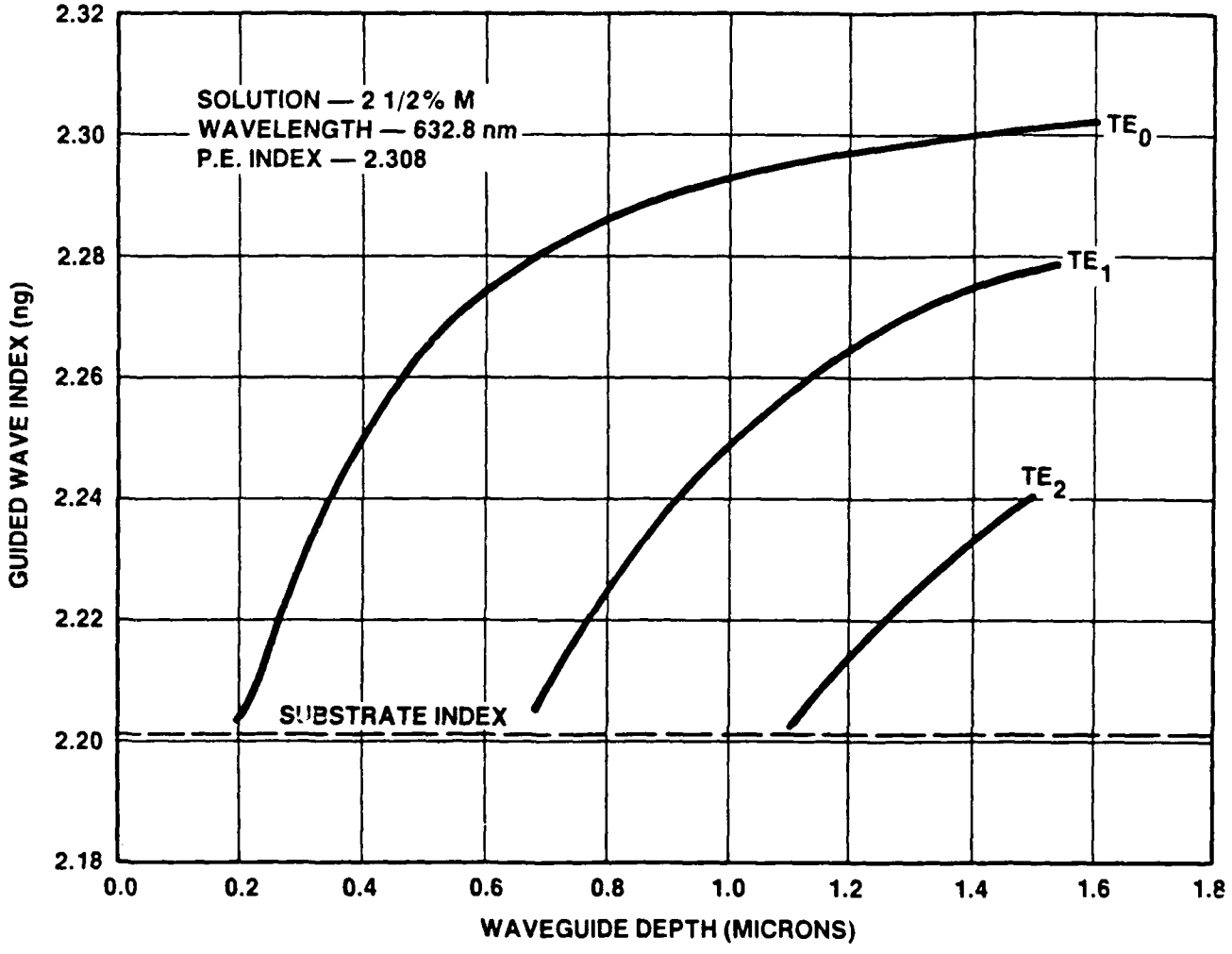

FIGURE 5. Dispersion curves for PE:$LiNbO_3$. The graph was calculated using a step index model and the measured surface index from guides fabricated in a 2.5%M lithium benzoate buffered solution.

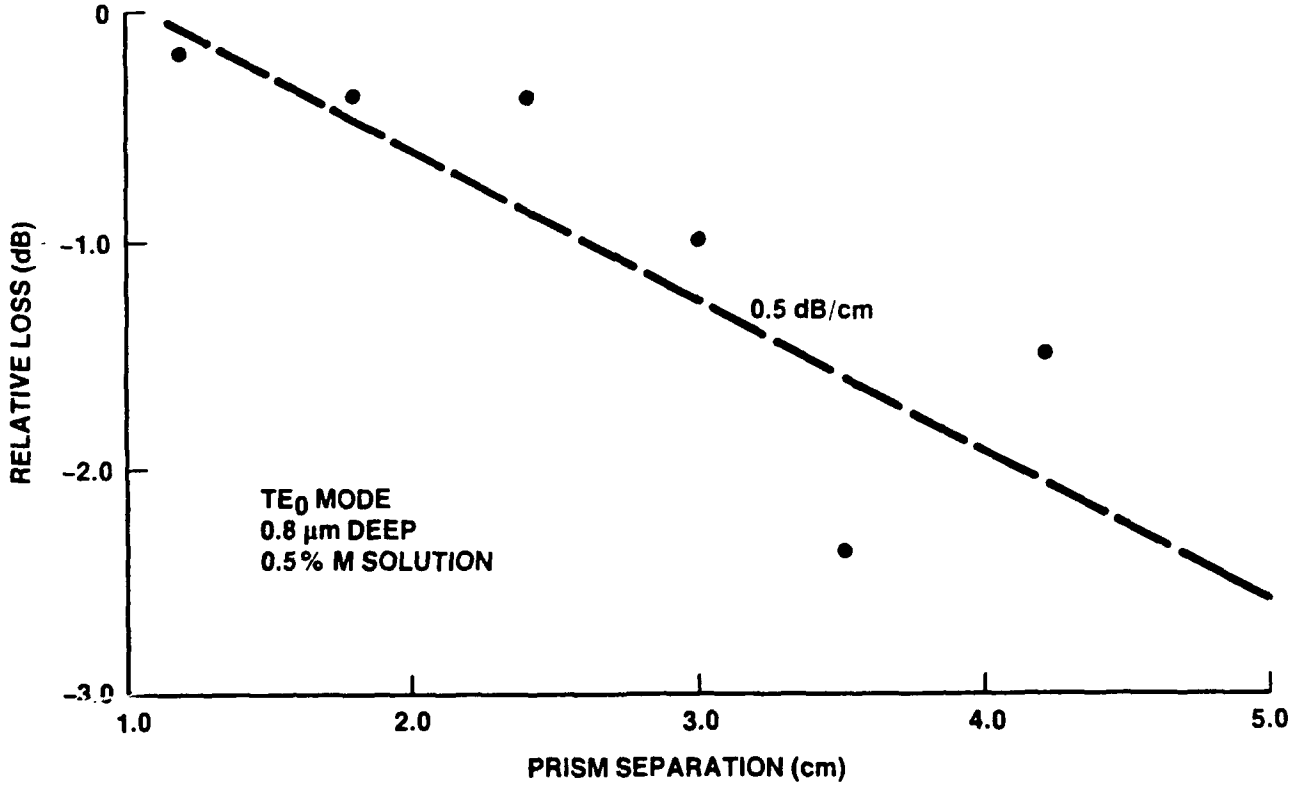

FIGURE 6. Propagation loss for a Y-cut PE:$LiNbO_3$ planar waveguide. The fundamental mode in a dual mode guide 0.8 microns deep was measured.

approximate loss of the TE_o mode to be 0.5 dB/cm. Optical loss and scatter in PE:$LiNbO_3$ waveguides are strong functions of the guided mode index as will be discussed later.

2. OPTICAL MEASUREMENTS AT = 832 nm

A GaAlAs laser diode source with the above prism coupled test set was used to measure the guided optical wave properties of two proton exchanged multimode waveguides for comparison with HeNe data. The m-line and light output were visualized with an infrared viewer. The calculated index and thickness of the two samples are shown in Table 2. The average index difference between the two wavelengths is .038. The average substrate index at the two wavelengths as measured on congruent $LiNbO_3$ is 2.2028 (λ=633 nm) and 2.1727 (λ=832 nm). This represents an index difference between the wavelengths of .030. The measured thickness of the diffused region at both wavelengths is the same within limits of experimental accuracy.

TABLE 2

Comparison of Optical Index and Exchange Depth for Multimode PE:$LiNbO_3$

	SAMPLE 1		SAMPLE 2	
WAVELENGTH (nm)	INDEX (n_e)	THICKNESS (μm)	INDEX (n_e)	THICKNESS (μm)
633	2.3123	2.480	2.3080	2.700
832	2.2726	2.410	2.2720	2.660

Infared optical propagation losses showed similar trends to those at the HeNe wavelengths. For guided modes with effective indices above 2.2500 the propagation loss was low. As the guided wave index decreased below this value the m-line broadened and there was a significant increase in loss (>20db/cm). The ordinary index, n_o, for $LiNbO_3$ at 832 nm is 2.2515. This indicates that conversion of the guided mode into the substrate mode is most likely the major cause of the increased loss.

3. WAVEGUIDE STABILITY

Early in the development of proton exchanged waveguides it was reported that there was a drift in the refractive index of the PE:$LiNbO_3$ with time.[9,10] Since most of the shift in refractive index occurred in a matter of days, stabilization was achieved by storage for a few weeks or by low temperature annealing. Jackel and Rice[1] identified the shift as due to the formation and subsequent relaxation of metastable phases and showed that the addition of lithium benzoate improves the stability. Stability of the waveguide index is extremely important in the design of Bragg cell devices.

The waveguides fabricated under this program, using 2.5 molar percent lithium benzoate, were measured periodically in time to determine changes in the waveguide indices. Single, double and triple mode guides were evaluated. The period of evaluation was from three to five months. On the samples tested the change in the extraordinary guided mode indices was less than 0.2% for the single mode guides and less than 0.1% for the dual and triple mode waveguides. The experimental accuracy of the measurements is approximately 0.1% and therefore the 2.5 molar percent guides are considered quite stable.

4. OPTICAL QUALITY OF PE:$LiNbO_3$ WAVEGUIDES

The objective of the optical waveguide development was to form a low-loss, low-scatter single mode waveguide by proton exchange. In order to obtain a highly efficient acoustooptic interaction in the 1.0 to 2.0 GHz region a proton exchange depth of approximately 0.5 μm was required. In earlier work at Motorola low-loss multimode waveguides had been obtained with proton exchange depths of approximately 0.7 μm and higher. It was anticipated that a higher buffer solution would permit shallower guides to be formed without degrading their optical quality.

A large number of single mode PE:$LiNbO_3$ waveguides were processed together with a few dual and multimode for reference purposes. Most single mode waveguides exhibited high loss and scatter levels causing the guided beam to fan out in the plane of the waveguide. This was dramatically different from the very confined light streak observed in

multimode waveguides and titanium indiffused waveguides. Qualitative light streak observations revealed that the optical loss-scatter behavior is mode index dependent. An examination of single, dual and multimode guides showed that if the guided mode index was above 2.28 or below 2.22 (approximately) there was good low loss optical propagation. Whereas, in the region of guided mode indices from 2.22 to 2.25 there was high loss and scatter and between 2.25 and 2.28 the loss and scatter of the light streak decreased. It was difficult to quantize these levels but it appeared that the transition at 2.22 was sharp while there was a more gradual improvement in waveguide quality as the mode index approached the 2.28 range. The optical quality continues to increase for higher mode indices but single mode propagation occurs only when the fundamental mode is below 2.28.

Evidently, both the optical and acoustic properties were adversely affected by the presence of a high concentration of hydrogen replacing the lithium. It was decided that a post processing furnace anneal was necessary both to change the concentration of the hydrogen and see if a reasonably high index, low-loss condition for optically guided modes could be achieved.

The following procedure allowed investigation of many annealing temperatures and durations. Multimode guides are annealed in increments of 5 minutes to several hours depending on the temperature. After each stage, the sample is cooled, optical quality observed, and guided wave indices measured. The index profile is plotted by the inverse-WKB method and the profile change analyzed. The anneal time for the next stage is then determined. Figure 7 shows that a proton exchanged multimode waveguide step index profile transitions into a tapered index profile due to annealing at 350^{o}C. (The same type of profile change is assumed in shallower guides but is difficult to varify with the WKB method since profile plots for guides with less than 4 modes are usually inaccurate.) Although the transition is faster at higher temperatures, the evolution of the index profile is very similar. The waveguide optical quality proved strongly dependent on the final distribution of hydrogen (i.e. final index profile) and not on the time and temperature of the anneal.

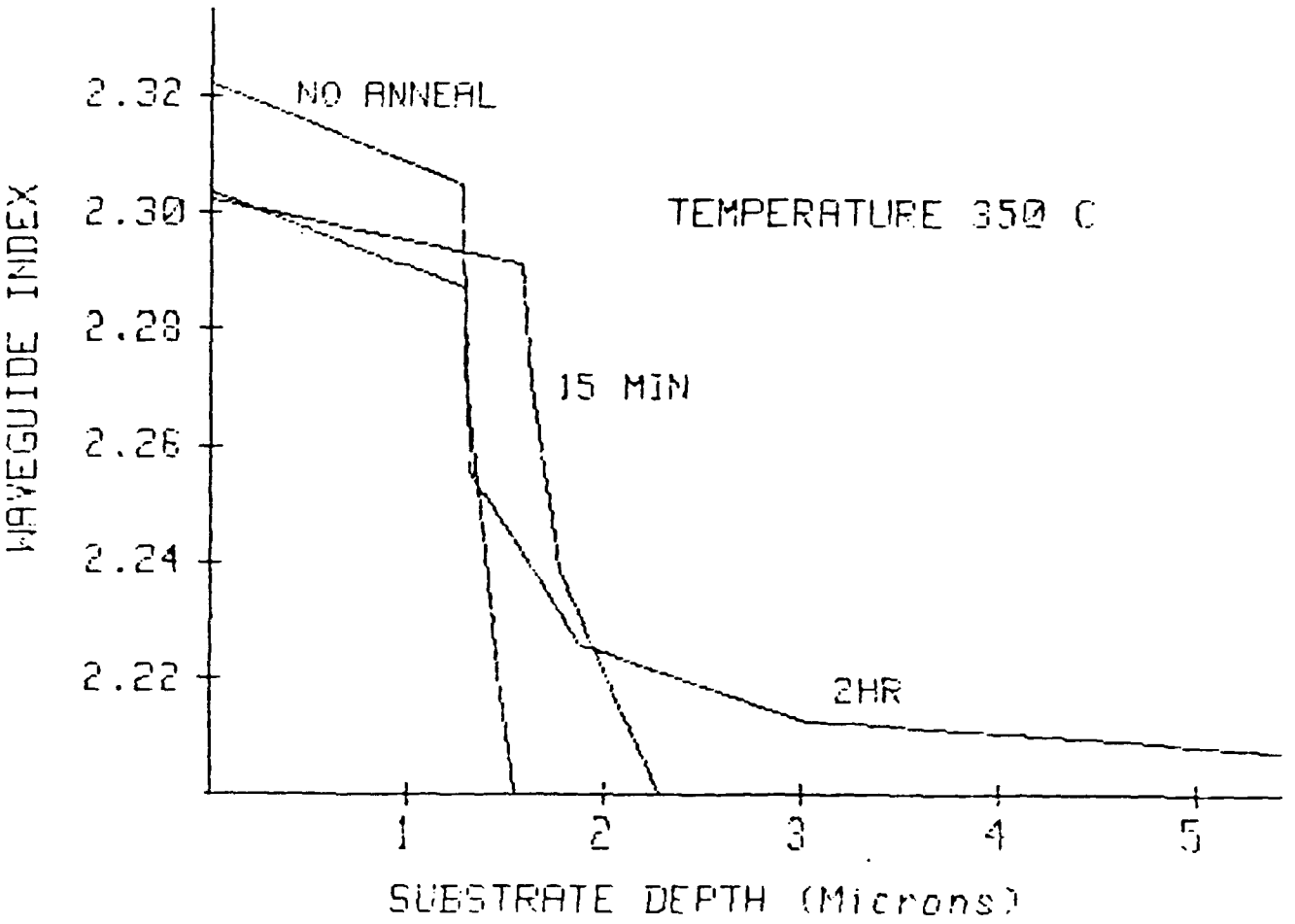

FIGURE 7. Index profiles for annealed PE:$LiNbO_3$. The original step index profile becomes tapered as hydrogen ions (protons) diffuse into the substrate.

Therefore, the temperature was chosen such that the anneal time was long enough to allow ease of profile control, yet short enough to minimize process time. Subsequently, many single and dual mode guides were annealed and optical improvements observed to determine the final parameters used to fabricate guides for the acousto-optic measurements.

The following guidelines were established for post proton exchange annealing. Substrates with a proton exchange depth in the range of 0.3 μm to 0.35 μm are used. The anneal is carried out at 350°C in an oxygen atmosphere for a period of approximately 45 minutes decreasing the guided mode index to approximately 2.22. The sample is measured optically and returned for additional annealing if the index, loss and scatter conditions are not met.

5. POLISHING OF MULTIMODE WAVEGUIDES

A series of multimode waveguides were surfaced polished to determine if surface roughness produced by the proton exchange process caused significant waveguide loss and scatter. Polishing was calibrated to accurately decrease the waveguide depth until single mode propagation occurs (<.64 microns). Guided mode index changes, propagation loss, and waveguide scatter characteristics were measured as the polishing proceeded. Optical quality of polished waveguides was essentially the same as the unpolished samples. For example, guided modes in polished waveguides having indices between 2.28 and 2.22 still exhibited high loss and scattering levels which, again, indicates a characteristic mode index dependence.

IV. ACOUSTIC MEASUREMENTS

1. INTRODUCTION

SAW transducer patterns were fabricated on YZ $LiNbO_3$ for acoustic evaluation of proton exchanged substrates at frequencies from 795 to 1450 MHz and 1.75 GHz. Standard photolithographic techniques were used for the lower frequency transducers and E-beam techniques for the higher frequency transducer. The fabrication and evaluation of E-beam transducer patterns was set aside early in the program when large acoustic losses were found at the lower frequencies. The decision was made to make a more quantitative assessment of the source of the losses which was better facilitated by the lower frequency measurements. More than 150 acoustic measurements were made on $LiNbO_3$ substrates fabricated under a variety of process conditions. The experimental conditions, results of measurements and analysis are discussed in the following paragraphs.

2. MEASUREMENT CONDITIONS

A SAW transducer array with center frequencies of 795, 895, 1020, 1190, 1340 and 1430 MHz was used. The transducers were broadband structures having between 6 and 12 electrode pairs at the five lowest frequencies and 22 pairs at the highest frequency. The separation between matched pairs was 1.9 mm. The transducer patterns were photolithographically replicated on the $LiNbO_3$ using a 700 Å aluminum layer. Three types of $LiNbO_3$ substrates were fabricated for measurement purposes: 1) unprocessed substrates, 2) completely proton exchanged substrates and 3) selectively exchanged substrates where only the propagation region between transducer pairs was proton exchanged. This permitted a separation of the effects of proton exchange on SAW transducer conversion loss and propagation loss. Individual SAW die were mounted in metal dual-in-line packages and connected with aluminum wirebonds. The unmatched loss vs frequency response was measured on a network analyzer in a 50-ohm test fixture. Impedance measurements of the four lower frequency patterns were made on die mounted to the lip of a 50-ohm connector connected with short wire

bonds.

The loss vs. frequency response provided information on changes in the total transmission loss and the center frequency under different proton exchange conditions. The coupling factor was calculated from both transmission loss and impedance measurements. The change in center frequency was used to determine changes in phase velocity.

3. EXPERIMENTAL RESULTS

Figure 8 illustrates experimental data resulting from transmission loss measurements on the various substrates processed. In this figure, transmission loss, including the two transducer conversion losses and propagation loss, is plotted as a function of frequency using data taken at the six center frequencies measured. Transducers operating on unprocessed $LiNbO_3$ substrates exhibit the lowest losses. These losses are close to measured values on titanium indiffused substrates. The loss is substantially higher for the three proton exchange depths shown and increases with exchange depth and with frequency in a completely proton exchanged wafer. The transmission loss is almost doubled as the exchange depth is doubled from 0.4 μm to 0.8 μm. The line identified as "masked" represents the transmission loss in the selectively exchanged substrates where the transducers were placed on a region of the $LiNbO_3$ that was not proton exchanged. The propagation path was across a region proton exchanged to a depth of 1.3 μm. The total transmission loss is within a decibel of that measured on the unprocessed substrates. The same loss measured when both transducers and path were over the 1.3 μm deep exchanged region was 55 dB at 1020 MHz. This leads to the conclusion that the propagation loss is not a major contributor to the observed transmission loss and that the large increase in PE substrates is primarily due to transducer conversion loss.

The SAW coupling coefficient, k^2, for each substrate type was calculated from the transmission loss measurements by normalizing to loss values for the unprocessed substrates and assuming that propagation losses can be neglected. The coupling coefficient was also determined independently from impedance measurements for a few selected substrates.

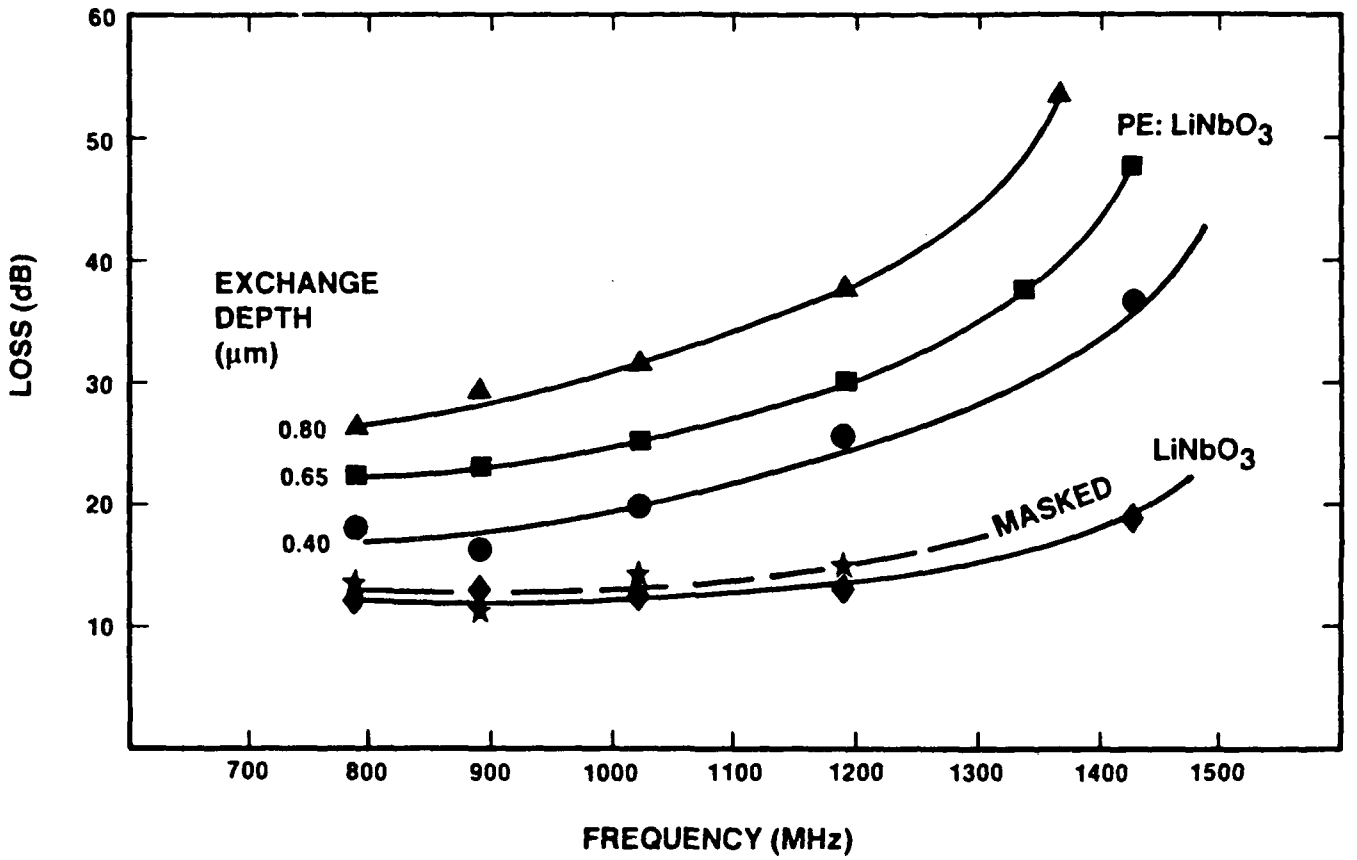

FIGURE 8. Transmission loss between SAW transducer pairs on proton exchanged YZ $LiNbO_3$.

Table 3 shows the k^2 coupling coefficient for three different proton exchange depths calculated from measured values of transmission loss and impedance at 794 MHz. The coupling factor values decrease with increasing proton exchange depth. The values calculated from the impedance measurements are substantially lower than those from transmission loss measurements. This difference is attributed to errors from parasitic effects which become significant at high frequencies.

TABLE 3

Calculated k^2 Coupling Coefficient at 794 MHz

for Proton Exchanged $LiNbO_3$

EXCHANGE DEPTH (μm)	IMPEDANCE MEASUREMENT k^2	TRANSMISSION LOSS k^2
0	.040	.045
0.59	.021	.033
0.90	.013	.022
1.18	.007	.020

4. ANALYSIS OF RESULTS

Davis[8] presented experimental evidence that suggested a degradation of the piezoelectric constants and increased SAW attenuation in proton exchanged $LiNbO_3$. The experimental evidence just described indicates a degradation of the piezoelectric properties but no major increase in propagation loss. Figure 9 presents calculated values of the k^2 coupling factor for several samples as a function of the proton exchange thickness to the surface acoustic wavelength ratio. Also shown on the figure is the predicted theoretical drop in the k^2 coupling factor for a piezoelectrically inactive proton exchanged region. Theoretically, the coupling factor decreases rapidly as the thickness to wavelength ratio increases. The measured coupling factor values follow the same trend as that expected for a piezoelectrically inactive region. Thus, the exchange of hydrogen for lithium alters $LiNbO_3$ properties to essentially negate the piezoelectric property. At this point, we

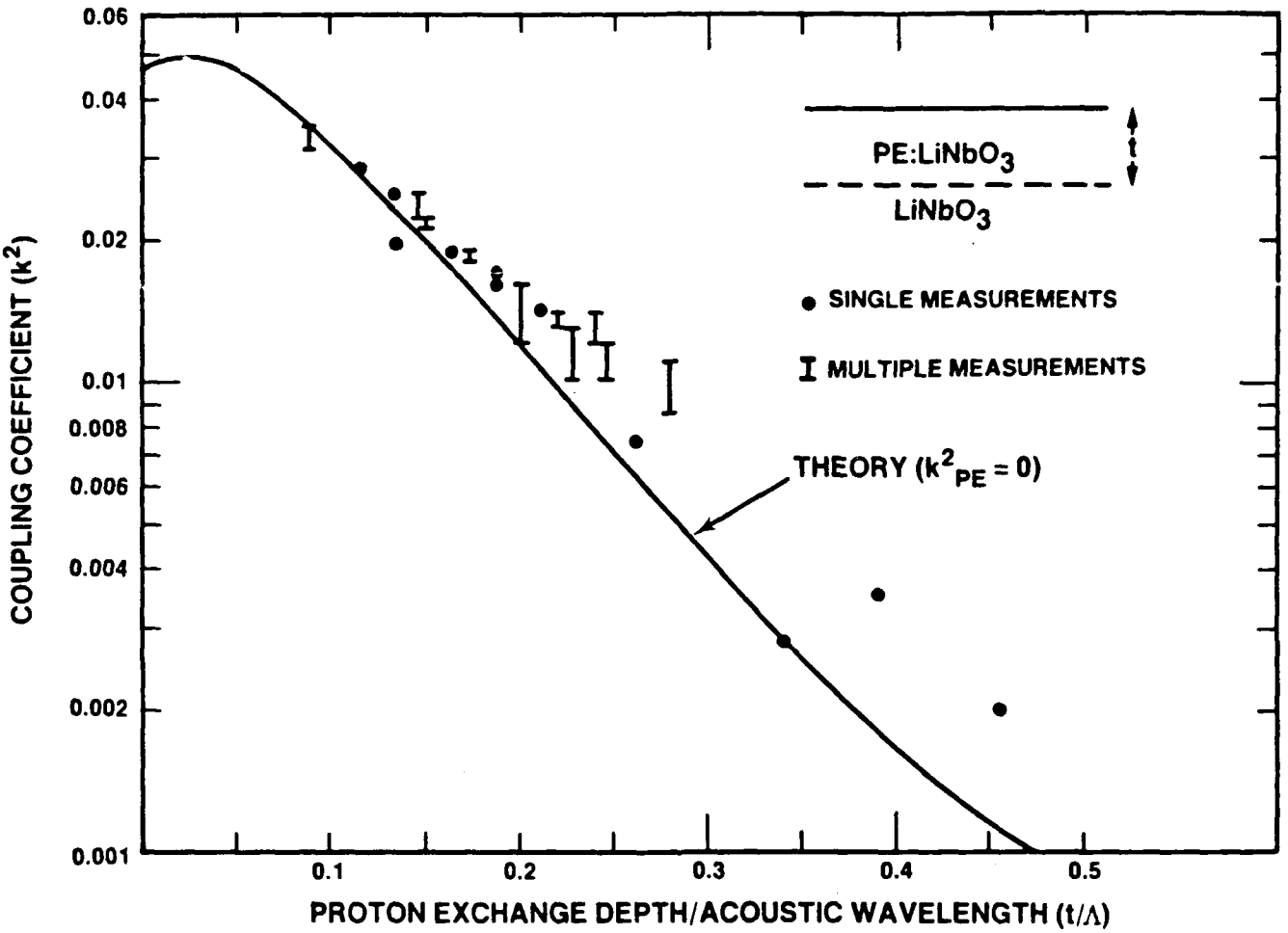

FIGURE 9. SAW coupling coefficient for PE:$LiNbO_3$. The solid line represents the theoretical k^2 contribution of the underlying substrate when the k^2 of the proton exchanged region is set to zero.

expected a reduction in acousto-optic activity since the electro-optic contribution will be substantially reduced because the piezoelectrically induced field is not present (Section V.4.).

It was expected that the piezoelectrically inactive region would also decrease the SAW velocity. Assuming no other crystal properties were altered, the phase velocity would lie between the theoretical values for a shorted and unshorted condition at the $LiNbO_3$ surface. The actual phase velocity in the proton exchange region was calculated from the measured shift in the transducer center frequency. Figure 10 shows the theoretical and experimental SAW phase velocities plotted against the proton exchange depth to acoustic wavelength ratio. The average SAW velocity in PE:$LiNbO_3$ is 1% below the theoretically predicted value based on the degradation of only the piezoelectric property. This suggests that the proton exchange process has also softened the elastic constant by about 2%, because theoretically, a change in the elastic constant produces half the change in velocity. These measurements are considered preliminary in nature and show some scatter since broadband transducers have been used and measurement accuracy is affected by irregular bandshapes and errors in transducer - crystal orientation.

5. ANNEALING EXPERIMENTATION

Furnace annealing of the proton exchanged substrates resulted in a marked decrease in transmission loss due to improved piezoelectric activity. Samples were annealed at 350°C for durations of 15 minutes to one hour. Table 4 gives an example of the transmission loss before and after annealing proton exchanged substrates. Optical measurements determined that substantial diffusion of hydrogen deeper into the substrate decreased the hydrogen density near the surface. This accounts for reductions in the transmission losses back to levels slightly higher than that of unprocessed substrates. The measured k^2 coupling coefficient for the annealed substrate lies between .033 and .035 which is 25% below the theoretical coupling coefficient.

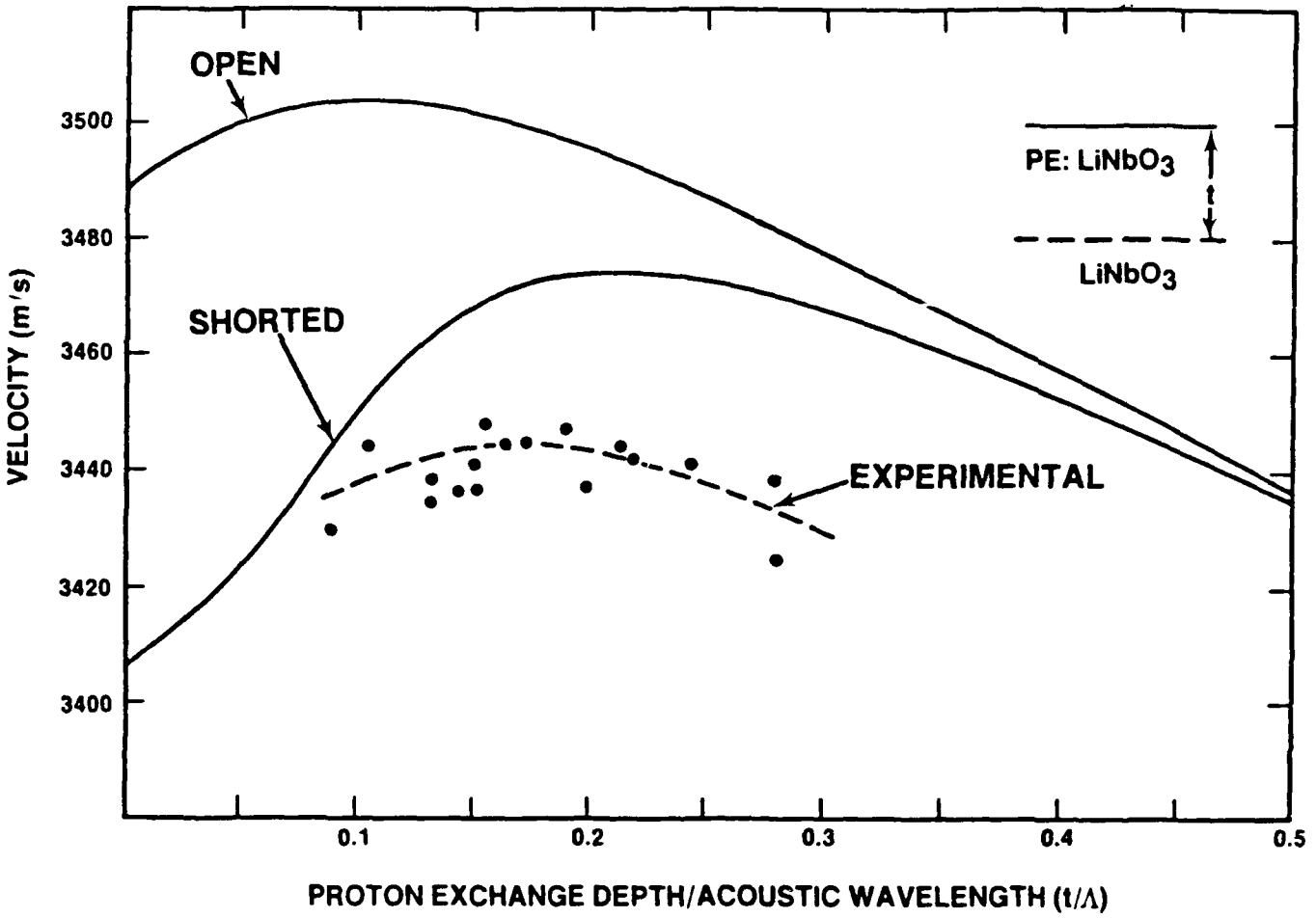

FIGURE 10. SAW phase velocity on YZ PE:$LiNbO_3$. The curve labeled shorted can be thought of as the theoretical SAW velocity in the presence of a metalized surface layer.

TABLE 4

SAW Transmission Loss Measurements for
Unannealed and Annealed Proton Exchanged
$LiNbO_3$ Substrates

FREQUENCY (MHz)	UNANNEALED LOSS (dB)	ANNEALED LOSS (dB)	COUPLING COEFFICIENT OF ANNEALED GUIDES (k^2)
795	24.0	17.0	.033
895	25.0	16.5	.033
1020	30.0	16.0	.035
1190	32.0	17.5	.035

V. ACOUSTO-OPTIC MEASUREMENTS

1. TEST SET-UP

Acousto-optic diffraction efficiencies for single transducer Bragg cells were measured utilizing the configuration shown in Figure 11. A Spectra-Physics model 159 helium-neon laser provides coherent light at 6328 Å. The randomly polarized output is linearly polarized, focused by a cylindrical lens, and coupled into the waveguide by a rutile prism. The parallel beam is centered between the transducer pair. The deflected beam and undeflected beam are prism coupled out and each intensity is measured with a Photodyne model 66XLA wide area silicon detector. The table consisting of the two coupling prisms clamped to the Bragg cell and electrical lead-in is mounted on a two axis rotatable stage for maximum optical coupling and Bragg interaction.

The SAW transducers are driven by a Hewlett Packard model 8614A RF signal generator and a linear amplifier. RF power is monitored through a -20dB directional coupler and delivered to the transducers via flexible coax, 50 ohm microstrip and aluminum wire bonds. There is no attempt to electrically match the transducer impedance.

2. MEASUREMENT PROCEDURE

The following describes the most convenient and expedient procedure for performing acousto-optic measurements. The best optical guides are selected for transducer patterning and wire bonding to the test fixture. After the coupling prisms are clamped to the waveguide, the acoustic insertion loss is measured with a network analyzer. Subsequently, the table is mounted to the two axis rotational stage and the laser beam is coupled into the waveguide. The transducer is driven at its center frequency and the device is tested at the Bragg angle for maximum acousto-optic diffraction. For devices with low diffraction efficiencies the RF is pulsed at 1 Hz to allow visual alignment of the photodetector to the diffracted beam.

Diffraction efficiency, defined as the diffracted beam intensity divided by the sum of the deflected and undeflected intensities, is measured and plotted for discrete values of CW acoustic drive power

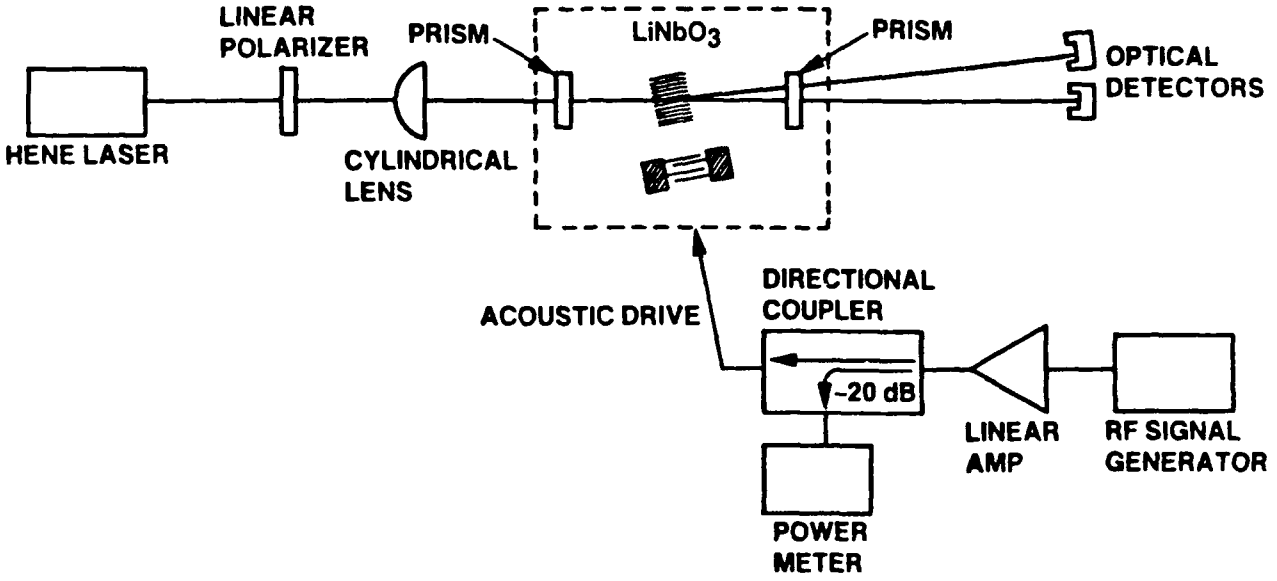

FIGURE 11. Test configuration for acousto-optic measurements.

(Figure 12). It is convenient to assign a single value of diffraction efficiency for a particular device for comparison purposes. In most IOSA applications transducers are driven at low power levels for operation in the linear region shown in Figure 12. Therefore, the slope of the curve in this region is usually considered the device efficiency and expressed in terms of percent light diffracted per watt (%/watt). Note, because the theoretical diffraction efficiency depends on the acoustic power (P_{ac}) as the $\sin^2 (A\sqrt{P_{ac}})$, slopes can exceed 100%/watt.

3. RESULTS AND OBSERVATIONS

a. Ti:$LiNbO_3$ Baseline

The primary goal of this investigation was to optimize the fabrication of proton exchanged waveguides to increase the AO diffraction efficiency of surface wave Bragg cells above levels shown by the existing technology. Therefore, the diffraction efficiency afforded by Ti:$LiNbO_3$ guides provided a reference for comparison with proton exchange results.

Bragg cells of Ti:$LiNbO_3$ were built very similar to PE Bragg cells for accurate comparisons of diffraction efficiencies. Titanium indiffused lithium niobate guides were fabricated by the method previously described in section II.3. Transducers were patterned on Ti guides using the same photomask and processing techniques. The devices with the lowest acoustic loss were then evaluated acousto-optically. Measured values of diffraction efficiency on these indiffused guides were substantially lower than expected. Instead of concentrating on duplicating previous AO results for Ti:$LiNbO_3$ it was decided that efforts would be focused on AO measurements of proton exchanged guides. Therefore, an alternate approach was taken for establishing a comparison reference.

Previously, measurements were performed at Motorola on Ti:$LiNbO_3$ Bragg cells made by identical methods using the same transducer photomask. Diffraction efficiencies were measured using 8230 Å light from a GaAlAs laser diode. A theoretical algorithm was used to convert

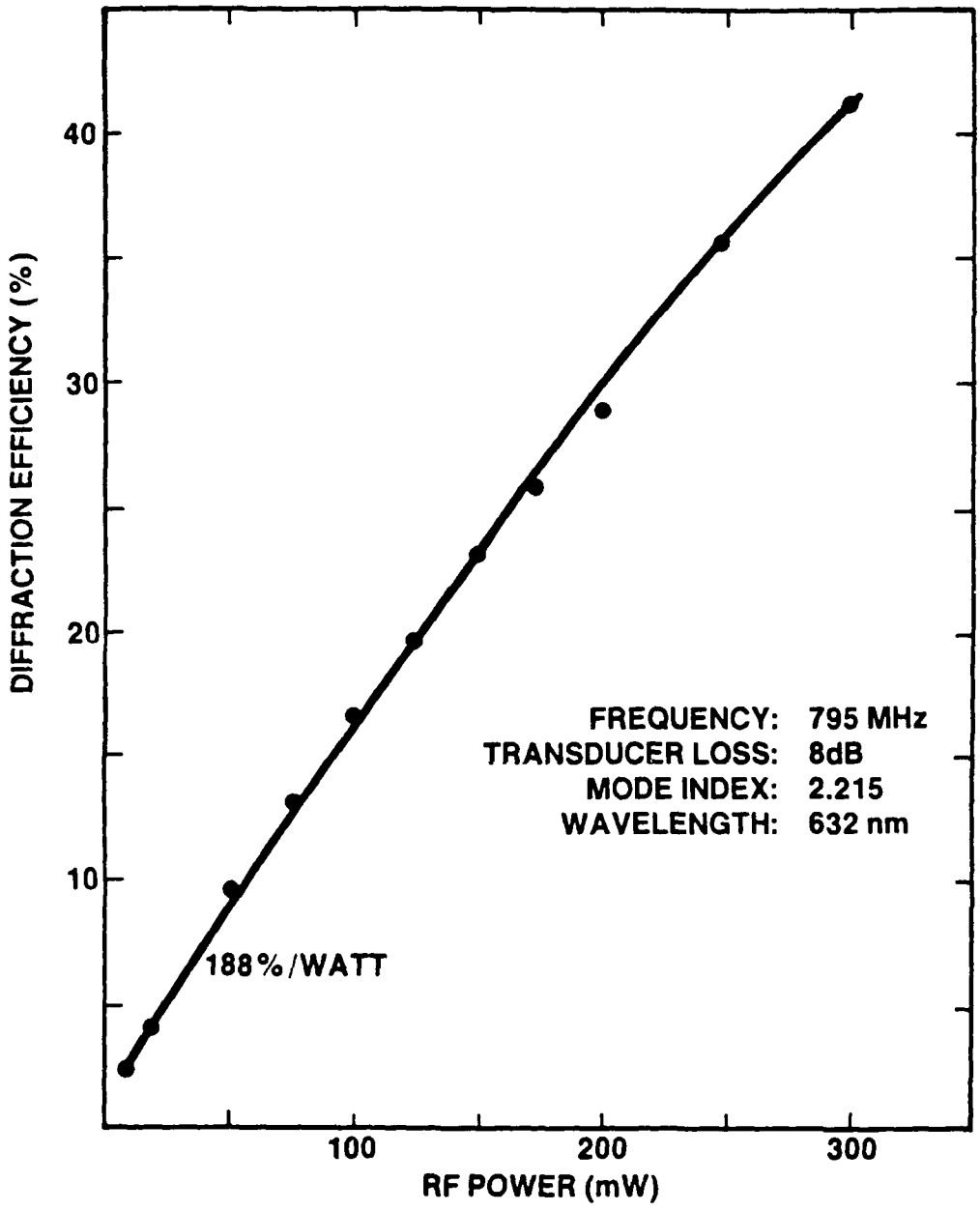

FIGURE 12. Diffraction efficiency of a PE:$LiNbO_3$ Bragg cell. The measured acousto-optic response was from a single transducer driven at its center frequency.

the measured results to corresponding values expected for the diffraction of 6328 Å laser light. The accuracy of this conversion was considered reasonable for purposes of comparison between the diffraction efficiencies of Ti:$LiNbO_3$ and PE:$LiNbO_3$.

b. Acousto-optic Measurements of PE: and TiPE:$LiNbO_3$

The best results of more than 20 measurements of the acousto-optic diffraction efficiency in PE: and TiPE:$LiNbO_3$ are shown in Table 5. The efficiency in Ti:$LiNbO_3$ at each frequency forms a baseline for comparison. The values are normalized for convenience to a single transducer loss of 10 dB. Diffraction efficiencies are expressed in percent per watt and asterisks indicate TiPE waveguides. Samples originally fabricated with a high optical guided wave index and then annealed to a low index exhibited diffraction efficiencies just below those of Ti:$LiNbO_3$. The high index unannealed samples which provide the best optical confinement showed suprisingly low diffraction levels.

TABLE 5

Acousto-Optic Diffraction Efficiency in %/Watt

		PROTON EXCHANGED	
FREQUENCY		LOW INDEX	HIGH INDEX
(MHZ)	Ti:$LiNbO_3$	ANNEALED	NO ANNEAL
794	117	92	5.1*
893	124	99*	6.9*
1021	75	52	-
1340	40	26	-

*TiPE:$LiNbO_3$ Waveguides

The best low index annealed guides were exchanged single mode with a guided mode index of 2.24 - 2.26 and then furnaced annealed from 45 - 75 minutes reducing the fundamental mode index below 2.225. Often this resulted in the formation of a second order mode. Figure 8 is a photograph of the output of a dual mode Bragg cell showing the two

53221-12

FIGURE 13. Photograph of an acousto-optically diffracted mode. The fundamental mode in a dual mode PE:$LiNbO_3$ Bragg cell is shown as the diffracted spot to the left.

undeflected orders and only the fundamental seen deflected. In all cases, only the diffraction efficiency of the fundamental was measured since the diffraction of higher order modes could not be detected.

A few observations drawn from the raw data are of interest. First, the diffraction efficiency depended strongly on the final waveguide index profile and fundamental mode index and not on the number of modes present in the waveguide. Secondly, the guides fabricated in a 1 M% lithium benzoate solution exhibited similar diffraction levels as compared to 2 .5 M% guides. The acoustical, optical and acousto-optic measured values of TiPE guides were very similar to those of PE guides. Finally, the higher optical quality waveguides provided better diffraction efficiency in almost every case.

4. THEORETICAL CONSIDERATIONS

Low acousto-optic diffraction efficiency exhibited by proton exchanged waveguides can be partially explained by examining the individual components that contribute to diffraction. It is well known that the efficiency of acousto-optic Bragg diffraction for a TE mode in YZ $LiNbO_3$ is directly proportional to the sine squared of the overlap-integral, Γ. This includes the contributions due to the acousto-optic (Γ_{ao}) and the electro-optic (Γ_{eo}) effects. White et al[11] showed that

$$\Gamma \cong \Gamma_{ao} + \Gamma_{eo}$$

and that

$$\Gamma_{ao} = r_{33} E_3(x_2)$$

where r_{33} is the electro-optic constant, E_3 is one of the electric-field components created by the SAW, and x_2 is the distance into the substrate. Acoustic measurements indicate (section IV.4.) that piezoelectric activity has been severly reduced in the proton exchanged region. Therefore, it follows that E_3 is reduced and the electro-optic contribution to diffraction is reduced accordingly. Since the electro-optic effect dominates at high acoustic frequencies an observed decreased in acousto-optic diffraction efficiency is expected.

VI. CONCLUSIONS AND RECOMMENDATIONS

Proton exchange is a simple, well controlled, low temperature process for increasing the surface refractive index of $LiNbO_3$. The resulting high index waveguides exhibit excellent temporal stability when fabricated in a 2.5 M% lithium benzoate buffered solution. The optical quality of PE:$LiNbO_3$ waveguides proves strongly dependent on the guided index of the propagating mode. Acoustic experimentation revealed that proton exchange severely reduces the k^2 coupling coefficient, decreases the SAW velocity, and slightly increases the SAW propagation loss. These observations correlated with the theoretical model indicate a softening of the elastic property and, most importantly, an inactive piezoelectric property. Low acousto-optic diffraction efficiency of unannealed PE:$LiNbO_3$ Bragg cells was evidently caused by poor optical quality waveguides and the absence of a piezoelectrically induced electric field to produce the electro-optic contribution.

The results of a fairly exhaustive annealing program of PE and TiPE guides indicate that reducing the hydrogen density in $LiNbO_3$ improves the optical quality, the piezoelectric property, and the acousto-optic diffraction efficiency. Annealing the initial step index profile of proton exchanged guides to a tapered index profile similar to that of indiffused guides virtually restores the original $LiNbO_3$ properties. The most important result is the measured acousto-optic diffraction efficiency of these annealed guides is similar to levels exhibited by titanium indiffused $LiNbO_3$.

The proton exchange process has disrupted the crystal structure in some form such as dislocation of atoms, interstitial atoms, or incomplete bonding between atoms. A thorough study of the structural changes of PE:$LiNbO_3$ will be required to fully explain the results obtained under this program. Specialized techniques such as reflected high energy electron diffraction (RHEED) or some other form of spectroscopy could be used to map out possible crystal deformations. This combined with a study of the kinetics associated with the PE process including hydrogen and lithium mobilities in the lattice would determine a theoretical model to estimate effects on the piezoelectric and electro-optic properties. A

variation of the PE process or, perhaps, a new technique would result that could achieve the original contract goals. One immediate possibility is proton exchanging previously out-diffused $LiNbO_3$. The addition of hydrogen in already vacated lithium sites may lead to less disruption of the crystal structure and, perhaps, preservation of the original $LiNbO_3$ properties.

VII. REFERENCES

[1] J.L. Jackel, C.E. Rice, and J.J. Veselka, "Composition control in proton-exchanged $LiNbO_3$," Electronic Letters, Vol. 19, p. 387, 12 May 1983.

[2] M. DeMicheli, "Nonlinear effects in TiPE-$LiNbO_3$ waveguides for optical communications," Journal of Optical Communications, Vol. 4, No. 1, p. 25, 1983.

[3] K.K. Wong, R.M. DeLaRue, and S. Wright, "Electro-optic waveguide frequency translator in $LiNbO_3$ fabricated by proton exchange," Optics Letters, Vol. 7, p. 546, November 1982.

[4] R.A. Becker, "Comparison of guided-wave interferometric modulators fabricated on $LiNbO_3$ via Ti indiffusion and proton exchange," Applied Physics Letters, Vol. 43, p. 131, 15 July 1983.

[5] R.L. Holman, D. Hicks, and J. Bush, "Laser power handling and electro-optic performance of proton exchanged lithium niobate waveguides," Proceeding of the SPIE, Vol. 460-19, Los Angeles, California, 24-25 January 1984.

[6] E.M. Korabler, Yu. L. Kopylov, and V.V. Proklov, "Acousto-optic investigations of proton-exchanged waveguides in $LiNbO_3$," Technical Digest of 1984 IEEE international workshop on integrated optical and related technologies for signal processing, Florence, Italy, 10-11 September 1984.

[7] A. Dawar, R.M. DeLaRue, G.F. Doughty, N. Finlayson, S.M. Al-Shukri, and J. Singh, "Acousto-optic techniques in integrated optics," Proceeding of the SPIE, Vol. 517-09, Los Angeles, California, 24-25 January 1984.

[8] R.L. Davis, "Acousto-optic Bragg Diffraction in Proton Exchanged Waveguides," Proceedings of the SPIE, Vol. 517, p. 74, 1984.

[9] J.L. Jackel and C.E. Rice, "Short and long-term stability in proton exchanged lithium niobate waveguides," Proceedings of the SPIE, Vol. 460, p. 43, 1984.

[10] Alfredo Yi-Yan, "Index instabilities in proton exchanged $LiNbO_3$ waveguides," Applied Physics Letters, Vol. 42, p. 633, 1983.

[11] J.M. White, P.F. Heidrich, and E.G. Lean, "Thin-film acousto-optic interaction in $LiNbO_3$," Electronics Letters, Vol. 10, No. 24, p. 510-511, 28 November 1974